JACS
JOURNAL OF THE AMERICAN CHEMICAL SOCIETY

ARTICLE

pubs.acs.org/JACS

Unconventional Kondo Effect in Redox Active Single Organic Macrocyclic Transistors

Jeong Tae Lee,[†,#] Dong-Hun Chae,[§,⊥,#] Zhongping Ou,[∥] Karl M. Kadish,[∥] Zhen Yao,[*,§] and Jonathan L. Sessler[*,‡]

[†]Department of Chemistry and Institute for Applied Chemistry, Hallym University, Chuncheon, Gangwon-do 200-702, Korea

[‡]Department of Chemistry and Biochemistry, 1 University Station-A5300, The University of Texas at Austin, Austin, Texas 78712-0165, United States

[§]Department of Physics, 1 University Station-C1600, The University of Texas at Austin, Austin, Texas 78712-0264, United States

[∥]Department of Chemistry, University of Houston, Houston, Texas 77204-5003, United States

Supporting Information

ABSTRACT: Cyclo[6]- and cyclo[8]pyrrole, two aromatic expanded porphyrins, were studied in a single-molecule transistor (SMT) setup. The analyses of these compounds allowed us to observe an uncommon absence of an even−odd effect in the Kondo resonance in discrete, metal-free organic macrocyclic compounds. The findings from the SMT measurements of these cyclopyrroles were in accord with those from cyclic voltammetry (CV) studies and theoretical analyses. These findings provide support for the notion that SMT measurements could be useful as a tool for the characterization of similar types of aromatic macrocyclic compounds.

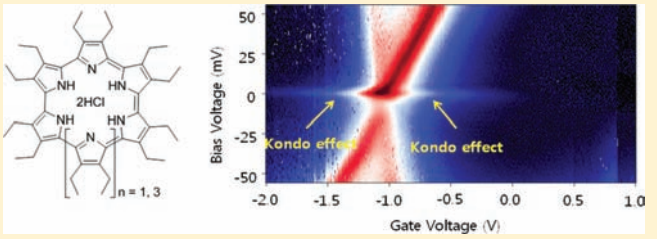

INTRODUCTION

Efforts to explore the behavior of individual single molecules, rather than an ensemble average of molecules, have prompted an increasing focus on so-called single-molecule spectroscopy (SMS). Recently, SMS has been applied to diverse fields of science, especially to material science[1] and biology.[2] SMS studies of polymers,[3] C_{60},[4] linear oligomers,[5,6] organic molecules,[7,8] metal coordinated complexes,[9,10] proteins,[11,12] and nucleic acids[13,14] have been reported. Because SMS refers to a variety of spectroscopic methods for the study of single molecules, a wide range of approaches have been exploited. For example, fluorescence−voltage measurements,[1b] confocal microscopy,[8] atomic force microscopy,[15] fluorescence resonance energy transfer,[16] fluorescence correlation spectroscopy,[17] single-molecule transistor (SMT) measurements,[18] scanning tunneling microscopy,[19] near-field scanning optical microscopy,[20] and Raman spectroscopy[21] have all been utilized for SMS. Among these techniques, SMT measurements are attractive for several reasons. First, the number of electrons can be easily controlled to investigate a redox state of a single molecule; second, the exchange coupling between the localized spin in an island (single-molecule) and the delocalized electrons in electrodes can be tuned by changing the gate voltage (Figure 1).

The Kondo effect[22] results from the entanglement between a localized spin and delocalized conduction electrons in a reservoir, for example, metal electrodes in a transistor, and leads to enhancement in conductance at zero-bias in single-electron transistors (SETs). Using recently developed SMT methods, it proved possible to observe the Kondo effect in carbon nanotubes,[23,24] metal complexes,[25,26] C_{60},[27] and in a conjugated linear oligomeric system.[5] However, as yet observations of the Kondo effect in discrete metal-free organic systems have been limited. Moreover, the metal-free carbon-containing systems studied to date have been endowed with special characteristics. C_{60}, for instance, lacks the C−H bonds typically found in organic compounds. In the case of the conjugated linear oligomeric molecule where the Kondo effect was observed,[5,28] the nature of the lowest unoccupied molecular orbital (LUMO) allows for the formation of an excited diradical state, which puts an unpaired electron at each end of the molecule and provides a clear path for electron flow.[29] We thus sought to explore whether the Kondo effect could be observed in simple, redox active aromatic macrocycles. As detailed below, this goal has now been achieved using two different expanded porphyrins, cyclo[6]pyrrole **1** and cyclo[8]pyrrole **2** (Figure 2).

Cyclo[6]pyrrole **1** ([22]hexaphyrin (0.0.0.0.0.0))[30] has a 22 π-electron aromatic periphery, whereas cyclo[8]pyrrole **2** ([30]octaphyrin(0.0.0.0.0.0.0.0))[31] has a 30 π-electron aromatic periphery. These cyclo[n]pyrroles may be considered as larger analogues of porphyrins, in that they are flat, symmetrical, and aromatic. However, relative to typical metal-free porphyrins, cyclo[n]pyrroles possess several more readily accessible oxidation states. Electrochemical studies of **1** and **2** have been carried out using cyclic voltammetry (CV). They revealed that the energy gap between the highest occupied molecular orbital

Received: September 19, 2011
Published: October 27, 2011

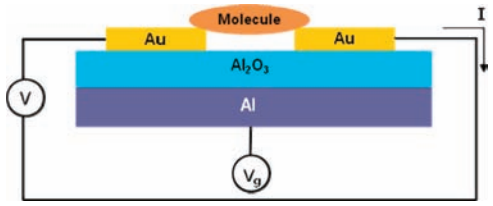

Figure 1. Schematic diagram of an SMT device. After spin-depositing cyclo[6]pyrrole or cyclo[8]pyrrole dissolved in dichromethane, the device is fabricated in situ using electromigration with a gold nanowire at 4.2 K. The charge state of a molecule is controlled by the aluminum gate, which has a strong capacitance coupling through a thin natural oxide layer.

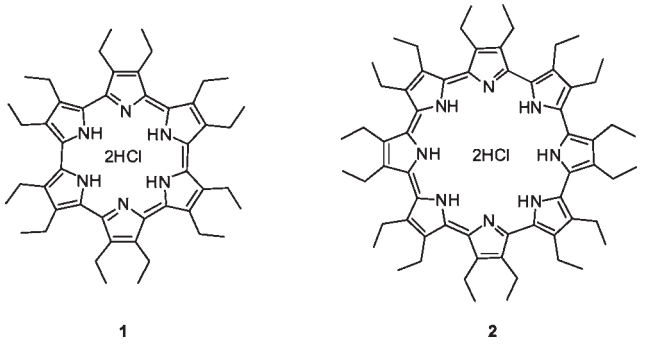

1 2

Figure 2. Cyclo[6]pyrrole **1** and cyclo[8]pyrrole **2** studied as single-molecule transistors.

(HOMO) and the LUMO is smaller than that of porphyrins, and that as the size of the expanded porphyrin increases, the HOMO−LUMO separation decreases.[30] Both **1** and **2** undergo a two-electron reduction event at room temperature. However, at low temperature (−70 °C), the two-electron reduction process can be resolved into two successive one-electron steps in the case of **1** (Figure 3).

Theoretical calculation predicts that both **1** and **2** have a degenerate HOMO and a strongly split LUMO pair, which has been confirmed by magnetic circular dichroism studies.[32] Recently, cyclo[6]- and cyclo[8]pyrroles were used for field-effect transistors based on Langmuir−Blogdett films; they showed high hole mobilities and high on/off ratios.[33,34] Because of these unique characteristics, we envisioned that cyclo[*n*]pyrroles **1** and **2** might be good candidates with which to investigate redox chemistry effects at the single-molecule level. In addition, it was considered that comparisons between CV data and SMT data could reveal differences and similarities between the two measurement methods. A close examination of the findings obtained from these disparate techniques could also reveal whether SMT is a viable characterization method for expanded porphyrins and by inference other conjugated organic species.

EXPERIMENTAL SECTION

Single-Molecule Transistor (SMT) Measurement. A schematic representation of the SMT setup used is shown in Figure 1. The devices themselves were fabricated on oxidized silicon substrates. Thin gold nanowires with narrow constrictions of approximately 100 nm and thicknesses of approximately 15 nm were patterned by electron-beam lithography on top of aluminum gates that have a thin aluminum oxide

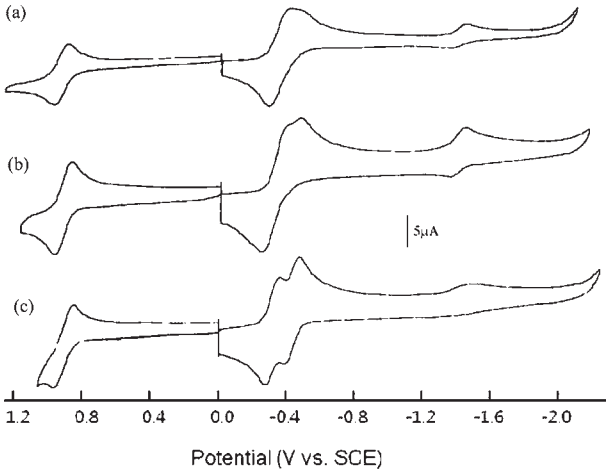

Figure 3. Cyclic voltammograms of cyclo[6]pyrrole **1** in CH_2Cl_2, 0.1 M TBAP at (a) room temperature, (b) −70 °C, and (c) −70 °C with TBACl added. As seen in the figure and noted in the text, two-electron reductions occur readily for cyclo[6]pyrrole at room temperature, but when cyclo[6]pyrrole was reduced at −70 °C in the presence of TBACl, two successive one-electron reduction waves could be resolved. For cyclic voltammetry experimental details, see the Supporting Information, section S1. SCE = saturated calomel electrode.

layer. After the nanowires were cleaned in oxygen plasma, a dilute cyclo[*n*]pyrroles in dichloromethane was spin-deposited on the substrates. The samples were then cooled to 4.2 K, and the Au nanowires were broken using the electromigration technique to create nanometer-sized gaps;[35] this was done by increasing the dc voltage across the wires while monitoring the resistance. The breaking process was generally terminated when the resistance across the wires increases above approximately 100 kΩ. Most of the devices produced in this way displayed a series of discrete resistance steps during the electromigration process and showed simple tunneling current with either no gate dependence or no measurable current. Such observations could be rationalized in terms of no discrete molecules bridging the gaps in these devices or the gaps being too large. A few devices showed tunneling through a multigrain system, a finding ascribable to a few cyclo-[*n*]pyrroles being connected via a tunneling link.[36,37] Several of the devices were characterized by saturating resistance plateaus with respect to the applied voltage (for details, see the Supporting Information, section S2); these devices generally exhibited voltage gaps in the current−voltage ($I-V$) curves that could be modulated with a gate voltage. The ability to effect such modulation is attributed to the presence of molecules in the nanogaps. For these devices, which were considered useful for probing the Kondo effect, conductance was measured in detail as a function of bias and gate voltages by numerically differentiating dc $I-V$ curves at different gate voltages. Among those devices, about 25% (7 of 28) exhibit an anomalous Kondo resonance as detailed below.

RESULTS AND DISCUSSION

We have found that Kondo resonance peaks appear on both even and odd charge states in transistors made up from single cyclo[*n*]pyrrole molecules. The observation of zero-bias Kondo resonance appearing in both even and odd (adjacent) charge states of a SMT has been observed previously.[38] However, it cannot be well described by the conventional spin 1/2 Kondo effect based on the Anderson impurity model.[39] Therefore, to provide a framework for our own findings, we considered a simple operational model: When exchange interaction within a molecule is comparable to the energy level spacing in the

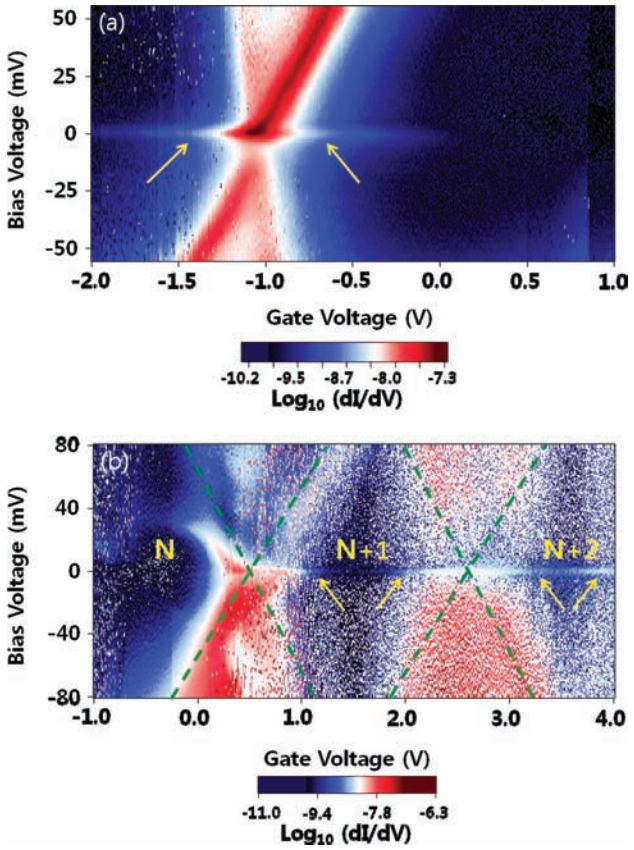

Figure 4. Differential conductance plotted on a logarithmic scale versus the bias and gate voltages measured at 4.2 K in SMTs incorporating cyclo[6]pyrrole **1**. (a) Conductance mapping of device A. Note that zero-bias conducting peaks (yellow arrows) appear in two Coulomb diamonds consecutively. (b) Conductance mapping of device B. The comparable peaks (yellow arrows) at zero-bias appear in the middle and right Coulomb diamonds. On the other hand, the zero-bias peak disappears in the left Coulomb diamond. We assign the number of electrons N, $N + 1$, and $N + 2$ from left to right, respectively. The two green dashed lines are drawn to help illustrate the boundary between the Coulomb blockaded regions and the conductance regions. The charging energy determined by the size of the blockaded region is about 100 meV.

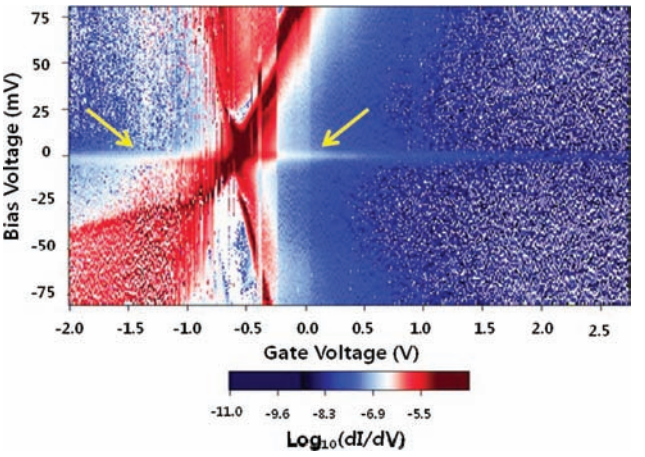

Figure 5. Two-dimensional differential conductance plot of a cyclo[8]pyrrole **2** device as a function of bias and gate voltages measured at 4.2 K. Similar zero-bias conducting peaks (yellow arrows) are observed.

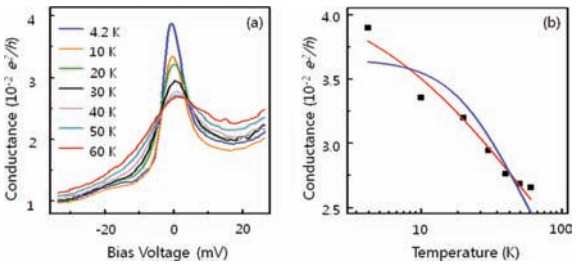

Figure 6. (a) Temperature dependence of zero-bias resonance. (b) Zero-bias conductance as a function of temperature. The zero-bias conductance decreases as the temperature increases. A logarithmic temperature dependence for the zero-bias peak is observed. The experimental points (■) were taken at a gate voltage of −0.5 V using device A presented in Figure 4a based on cyclo[6]pyrrole **1**. The red and blue lines represent fits to an empirical formula used by Parks et al.[40b] for the spin 1/2 Kondo model (blue trace) and the spin 1 Kondo model (red trace).

molecule, two successive electrons of the same spin may be added instead of in the form of an alternating spin-up and spin-down configuration in a pair. To the extent this model is valid, it leads to the prediction that Kondo resonances will be observed in two consecutive Coulomb diamonds. This is in fact what is seen in the case of devices constructed using macrocycle **1** (Figure 4).

Figure 4a shows a color plot of the differential conductance on a logarithmic scale as a function of bias and gate voltages for a device incorporating cyclo[6]pyrrole **1** (device A). Dark blue regions are Coulomb blockade regions (nonconducting areas), and red colors correspond to high conductance regions. A key feature of this device is that through capacitance coupling between the gate and the molecule, we can add or subtract electrons one by one to/from an individual molecule of cyclo[6]-pyrrole **1** connected to the source and drain gold electrodes by tunnel barriers. In Figure 4a, there exists a degeneracy point between what are two distinct charge states; these differ by the charge of a single electron, as is typically observed in an SET. The number of electrons present in the molecule increases (or decreases) one by one whenever the gate voltage passes by a degeneracy point in the positive (or negative) direction. However, the initial neutral charge state, and hence the charge on the molecule at any given gate voltage, cannot be determined independently because it depends on the local electrostatic environment. Remarkably, zero-bias resonances (ZBRs, yellow arrows) appear on both sides in two adjacent Coulomb blockaded regions. It was clearly observed that the suppression of conductance due to the Coulomb blockade effect is overcome at zero-bias. In addition, the ZBRs display strong gate dependence, because the features fade out as the gate voltage moves farther away from the degeneracy point.

Figure 4b shows the conductance mapping of another device derived from cyclo[6]pyrrole **1** (device B). In this case, three charged (redox) states are accessible within the gate range. If we assign N as the number of electrons in the molecule in the Coulomb diamond on the left of this plot, the middle and right Coulomb diamonds correspond to $N + 1$ and $N + 2$ charged states, respectively. While the N charged states show the conventional Coulomb blockade effect, ZBRs (yellow arrows) are observed in the middle ($N + 1$ charged state) and right ($N + 2$ charged state) Coulomb diamonds. Similar ZBRs were also observed in a device derived from cyclo[8]pyrrole **2**, as shown in Figure 5. The features are qualitatively similar to those of device

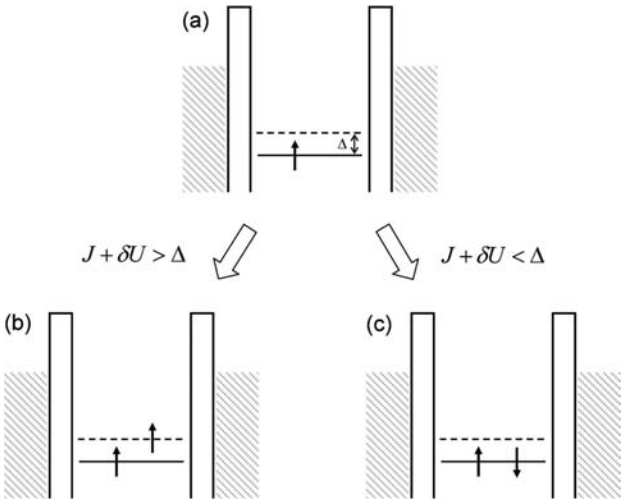

Figure 7. Schematic diagrams of state filling involving two added electrons. Two possible processes are available depending on the relationship between several energy factors, the exchange energy J, the extra Coulomb energy δU required to put two electrons in a single quantum state, and the energy level spacing, Δ, between molecular orbitals. When $J + \delta U > \Delta$, the second electron fills the next level to produce a spin-triplet state (a → b), a result that can explain the absence of even−odd parity effect. In contrast, a spin-up and spin-down paired electron state results when $J + \delta U < \Delta$ (a → c); this represents the case for the simplest Kondo effect due to spin 1/2.

A. It is believed that the redox states observed in device A correspond to the $N + 1$ and $N + 2$ charged states seen in device B. We note that none of 60 control devices prepared without any molecules being deposited displays the observed zero-bias features (for details, see the Supporting Information, section S3).

The temperature dependence of the ZBR for a device containing cyclo[6]pyrrole **1** that displays zero-bias conducting peaks across a degeneracy point has been measured (Figure 6). These data are obtained at gate voltage of −0.5 V for the device A presented in Figure 4a. In this case, logarithmic temperature dependence for the zero-bias peak is observed. This is a hallmark of a Kondo resonance feature and provides support for the notion that this feature results from a Kondo effect. The strong gate dependence of the ZBR is also consistent with the Kondo resonance.

To estimate the Kondo temperature at the given gate voltage, the temperature dependence was fitted to an empirical formula used by Parks et al.[40b] for the spin 1/2 Kondo model (blue trace) and the spin 1 Kondo model (red trace).[41] The observed nonsaturating behavior of conductance with decreasing temperature is consistent with an even charge Kondo effect with a spin = 1.[38,40b] The resultant Kondo temperature is about 130 K.

In systems with a simple spin 1/2 Kondo effect, the Kondo resonance disappears as the number of electrons is changed from odd to even. Obviously, this is not the case for the devices produced from **1** and **2**. Previous electrochemical studies have served to show that two-electron reductions occur readily for both **1** and **2**.[30] However, when **1** was electrochemically reduced at low temperature (−70 °C), two successive one-electron reduction processes could be resolved (Figure 3c). Such a finding leads us to suggest that there are very closely spaced LUMOs in **1** and, perhaps, **2**. Theoretical analyses based on DFT calculations also reveal the presence of two split LUMOs.[32] Thus, a key feature of the cyclo[n]pyrroles used in this study is that they provide a well-defined framework wherein device-scale Kondo effects can be related to bulk measurement features (e.g., electrochemistry), as well as molecular orbital theory. On the basis of a combination of theory and electrochemical experiment, it is believed that the closely spaced cyclo[n]pyrrole (n = 6 or 8) LUMOs are populated one by one during these SMT experiments.

Given the above, a model is suggested to account for our observations. Figure 7a displays the lower LUMO occupied by a first electron added from the electrode. This situation satisfies the condition of the Kondo resonance due to the spin 1/2. For the next reduced state, a significant charging energy is required to add one more electron to the molecule.

Electron−electron interactions play an important role in mediating Kondo effects in the single electron tunneling regime. Previous experimental evidence, involving the study of quantum dots based on two-dimensional electron gases,[42] as well as carbon nanotube transistors,[23] served to reveal that when exchange interactions dominate in systems with closely spaced energy levels, Kondo resonances can be observed for states with an even number of electrons. Such observations are not consistent with the constant interaction model, wherein electron−electron interactions are thought to be independent of the number of electrons.[43] Rather, these systems appear to follow Hund's rule as applied to atomic and molecular ensembles.

In addition, consideration must be made of several other energetic factors that determine how states are filled with extra electrons. For instance, one must account for (1) the exchange energy J that reflects the fact that the parallel spin configuration has a lower energy than an antiparallel one, (2) the energy level spacing, Δ, between the molecular orbitals, and (3) the extra Coulomb energy, δU, needed to put two electrons into a single quantum state. There are two possible scenarios, when $J + \delta U > \Delta$, and when $J + \delta U < \Delta$. Under the first of these, the second electron occupies the next level with a spin-triplet state (Figure 7a → b). By contrast, when $J + \delta U < \Delta$, electrons enter into the lower level consecutively in a spin-up and spin-down manner (Figure 7a → c).

To a first approximation, if the exchange interaction is significant as compared to the spacing between levels, the spin state is a triplet. Thus, a Kondo effect is still possible in a system with an even number of electrons because the net spin is 1. On the other hand, if the exchange interaction is negligible as compared to the level spacing, the total spin is zero. Therefore, no Kondo effect is expected. While the conventional spin 1/2 Kondo effect follows the second scenario (Figure 7a → c), the ZBRs seen in two adjacent Coulomb diamonds in our SMTs are best explained by the first scenario (Figure 7a → b).

The qualitative model given in Figure 7 provides a reasonable explanation for the data sets obtained during the present SMT studies. On the basis of the first scenario (Figure 7a → b), the observed ZBRs of cyclo[6]pyrrole **1** and those of cyclo[8]pyrrole **2** are easily rationalized. Disappearance of the ZBR in device B in the N charged state shown in Figure 4b can also be interpreted reasonably as follows: Previous theoretical studies based on symmetry arguments revealed that the HOMOs are degenerate in the neutral charged state.[32] Thus, these degenerate HOMOs should be filled with paired electrons with zero net spin. That is, no Kondo resonance is expected. Addition of a first electron then leads to a spin 1/2 state in a LUMO, resulting in the appearance of the Kondo resonance. Upon further reduction, the next electron occupies a different, albeit closely spaced, LUMO. This gives rise to a spin-triplet state, wherein a Kondo resonance still occurs, despite the fact that there are even numbers of electrons.

As a result, the ground spin state of device B can be described by the sequence of $S = 0 \rightarrow 1/2 \rightarrow 1$. This simple process can account for the observed features in Figure 3b. However, the suggested model and the given data are not enough to determine all of the underlying energy values, such as the exchange energy J, the excess Coulomb energy δU, and the energy level spacing Δ.

CONCLUSIONS

In summary, an unconventional Kondo effect, the appearance of Kondo resonances at zero-bias for the states containing both odd and even numbers of electrons in the SMTs of cyclo[n]pyrroles, has been observed. The present findings are readily explained by invoking a model wherein a strong exchange interaction within the molecule leads to Hund's rule behavior with the formation of a spin-triplet, which is energetically more favorable than the production of a singlet spin state. While qualitatively correct, this explanation and the underlying experimental data do not suffice for a detailed quantitative description. Further theoretical and experimental studies are needed if a more detailed understanding is to be obtained. Nevertheless, this study is highly informative in terms of confirming the accessibility of multiple electronic states within a set of well-defined aromatic species.

As confirmed by electrochemical analysis, the cyclo[n]pyrroles used in the present study are redox active. In particular, electrons can be added to or removed stepwise from these systems, with the energy difference between the first oxidation and first reduction processes (the HOMO−LUMO gaps) being relatively small for both cyclo[6]pyrrole **1** and cyclo[8]pyrrole **2** (as compared, e.g., to porphyrins). As a consequence, we were able to make working devices with both **1** and **2**. Importantly, the SMT studies proved to be in good agreement with the CV measurements and with theoretical analyses involving the frontier orbitals. We thus propose that SMT analysis of small organic molecules could prove complementary to other techniques, such as CV, in terms of analyzing structure-related features, and could do so free of bulk effects. This technique provides unique information, particularly with regard to accessible oxidations states and intrinsic electronic features. This leads us to suggest that SMT analyses of other expanded porphyrins and other conjugated systems are warranted.

ASSOCIATED CONTENT

Supporting Information. Experimental section. This material is available free of charge via the Internet at http://pubs.acs.org.

AUTHOR INFORMATION

Corresponding Author

sessler@mail.utexas.edu; yao@physics.utexas.edu

Present Addresses

[⊥]Max-Planck-Institute for Solid State Research, Heisenbergstrasse 1, D-70569 Stuttgart, Germany.

Author Contributions

[#]These authors contributed equally.

ACKNOWLEDGMENT

This research was supported by the Hallym University Research Fund (2009(HRF-2009-208) to J.T.L.), Korea Ministry of Knowledge Economy (grant no. K00041-04 to J.T.L.), the NIH (CA 68682 to J.L.S.), and the Robert A. Welch Foundation (grant nos. E-680, F-1591, and F-1018 to K.M.K., Z.Y., and J.L.S., respectively).

REFERENCES

(1) (a) Lupton, J. M. *Adv. Mater.* **2010**, *22*, 1689–1721. (b) Barbara, P. F.; Gesquiere, A. J.; Park, S.-J.; Lee, Y. J. *Acc. Chem. Res.* **2005**, *38*, 602. (c) Jurow, M.; Schuckman, A. E.; Batteas, J. D.; Drain, C. M. *Coord. Chem. Rev.* **2010**, *254*, 2297.

(2) (a) Lord, S. J.; Lee, H. D.; Moerner, W. E. *Anal. Chem.* **2010**, *82*, 2192–2203. (b) Yang, H. *Curr. Opin. Chem. Biol.* **2010**, *14*, 3–9. (c) Tessmer, I.; Moore, T.; Lloyd, R. G.; Wilson, A.; Erie, D. A.; Allen, S.; Tendler, S. J. B. *J. Mol. Biol.* **2005**, *350*, 254.

(3) Thomsson, D.; Lin, H.; Scheblykin, I. G. *ChemPhysChem* **2010**, *11*, 897–904.

(4) Park, H.; Park, J.; Lim, A. K. L.; Anderson, E. H.; Alivisatos, A. P.; McEuen, P. L. *Nature* **2000**, *407*, 57.

(5) Kubatkin, S.; Danilov, A.; Hjort, M.; Cornil, J.; Bredas, J.-L.; Stuhr-Hansen, N.; Hedegard, P.; Bjornholm, T. *Nature* **2003**, *425*, 698.

(6) Xu, B. Q.; Li, X. L.; Xiao, X. Y.; Sakaguchi, H.; Tao, N. J. *Nano Lett.* **2005**, *5*, 1491.

(7) Lang, E.; Hildner, R; Engelke, H.; Osswald, P.; Würthner, F.; Köhler, J. *ChemPhysChem* **2007**, *8*, 1487–1496.

(8) Yoo, H.; Yang, J.; Nakamura, Y.; Aratani, N.; Osuka, A.; Kim, D. *J. Am. Chem. Soc.* **2009**, *131*, 1488–1494.

(9) Li, Z.; Li, B.; Yang, J.; Hou, J. G. *Acc. Chem. Res.* **2010**, *43*, 954–962.

(10) Liang, W.; Shores, M. P.; Bockrath, M.; Long, J. R.; Park, H. *Nature* **2002**, *417*, 725.

(11) Lu, H. P. *Acc. Chem. Res.* **2005**, *38*, 557.

(12) Hofmann, H.; Hillger, F.; Pfeil, S. H.; Hoffmann, A.; Streich, D.; Haenni, D.; Nettels, D.; Lipman, E. A.; Schuler, B. *Proc. Natl. Acad. Sci. U.S.A.* **2010**, *107*, 11793–11798.

(13) Ha, T. *Biochemistry* **2004**, *43*, 4055.

(14) Liu, K. J.; Brock, M. V.; Shih, I.-M.; Wang, T.-H. *J. Am. Chem. Soc.* **2010**, *132*, 5793–5798.

(15) Duwezi, A.-S.; Cuenot, S.; Jerome, C.; Gabriel, S.; Jerome, R.; Rapino, S.; Zerbetto, F. *Nat. Nanotechnol.* **2006**, *1*, 122–125.

(16) Algar, W. R.; Prigozhin, M. B.; Liu, B.; Krull, U. J.; Gradinaru, C. C. *Proc. SPIE* **2009**, *7386*, 73860J.

(17) Chen, J.; Irudayaraj, J. *ACS Nano* **2009**, 3, 4071–4079.

(18) (a) Perrine, T. M.; Smith, R. G.; Marsh, C.; Dunietz, B. D. *J. Chem. Phys.* **2008**, *128*, 154706. (b) Yu, L. H.; Keane, Z. K.; Ciszek, J. W.; Cheng, L.; Tour, J. M.; Baruah, T.; Pederson, M. R.; Natelson, D. *Phys. Rev. Lett.* **2005**, *95*, 256803. (c) Yamaguchi, H.; Terui, T.; Noguchi, Y.; Ueda, R.; Nasu, K.; Otomo, A.; Matsuda, K. *Appl. Phys. Lett.* **2010**, *96*, 103117.

(19) Qiu, X. H.; Nazin, G. V.; Ho, W. *Phys. Rev. Lett.* **2004**, *92*, 206102.

(20) Szymanski, C.; Wu, C.; Hooper, J.; Salazar, M. A.; Perdomo, A.; Dukes, A.; McNeill, J. *J. Phys. Chem. B* **2005**, *109*, 8543.

(21) (a) Kneipp, K.; Wang, Y.; Kneipp, H; Perelman, L. T.; Itzkan, I.; Dasari, R.; Feld, M. S. *Phys. Rev. Lett.* **1997**, *78*, 1667. (b) Nie, S. M.; Emery, S. R. *Science* **1997**, *275*, 1102.

(22) (a) Kouwenhoven, L.; Glazman, L. *Phys. World* **2001**, *14*, 33. (b) Scott, G. D.; Natelson, D. *ACS Nano* **2010**, *4*, 3560.

(23) Liang, W. J.; Bockrath, M.; Park, H. *Phys. Rev. Lett.* **2002**, *88*, 126801.

(24) Jarillo-Herrero, P.; Kong, J.; van der Zant, H. S.; Dekker, C.; Kouwenhoven, L. P.; De Franceschi, S. *Nature* **2005**, *434*, 484.

(25) Park, J.; Pasupathy, A. N.; Goldsmith, J. I.; Chang, C.; Yaish, Y.; Petta, J. R.; Rinkoski, M.; Sethna, J. P.; Abruna, H. D.; McEuen, P. L.; Ralph, D. C. *Nature* **2002**, *417*, 722.

(26) (a) Perera, U. G. E.; Kulik, H. J.; Iancu, V.; Dias da Silva, L. G. G. V.; Ulloa, S. E.; Marzari, N.; Hla, S.-W. *Phys. Rev. Lett.* **2010**, *105*, 106601.

(b) Dias da Silva, L. G. G. V.; Tiago, M. L.; Ulloa, S. E.; Roboredo, F. A.; Dagotto, E. *Phys. Rev. B* **2009**, *80*, 15543.

(27) (a) Yu, L. H.; Natelson, D. *Nano Lett.* **2004**, *4*, 79. (b) Pasupathy, A. N.; Bialczak, R. C.; Martinek, J.; Grose, J. E.; Donev, L. A. K.; McEuen, P. L.; Ralph, D. C. *Science* **2004**, *306*, 86.

(28) Osorio, E. A.; O'Neill, K.; Wegewijs, M.; Stuhr-Hansen, N.; Paaske, J.; Bjornholm, T.; van der Zant, H. S. J. *Nano Lett.* **2007**, *7*, 3336.

(29) MacDiarmid, A. G. *Rev. Mod. Phys.* **2001**, *73*, 701.

(30) Köhler, T.; Seidel, D.; Lynch, V.; Arp, F. O.; Ou, Z.; Kadish, K. M.; Sessler, J. L. *J. Am. Chem. Soc.* **2003**, *125*, 6872.

(31) Seidel, D.; Lynch, V.; Sessler, J. L. *Angew. Chem., Int. Ed.* **2002**, *41*, 1422.

(32) Gorski, A.; Köhler, T.; Seidel, D.; Lee, J. T.; Orzanowska, G.; Sessler, J. L.; Waluk, J. *Chem.-Eur. J.* **2005**, *11*, 4179.

(33) Xu, H.; Yu, G.; Xu, W.; Xu, Y.; Cui, G.; Zhang, D.; Liu, Y.; Zhu, D. *Langmuir* **2005**, *21*, 5391.

(34) Xu, H.; Wang, Y.; Yu, G.; Xu, W.; Song, Y.; Zhang, D.; Liu, Y.; Zhu, D. *Chem. Phys. Lett.* **2005**, *414*, 369.

(35) Park, H.; Lim, A. K. L.; Alivisatos, A. P.; Park, J.; McEuen, P. L. *Appl. Phys. Lett.* **1999**, *75*, 301.

(36) Danilov, A. V.; Golubev, D. S.; Kubatkin, S. E. *Phys. Rev. B* **2002**, *65*, 125312.

(37) Out of 260 cyclo[6]pyrrole devices prepared, 28 gateable devices were obtained, and an unconventional Kondo resonance was seen in seven and out of these 28 gateable devices. Five out of 28 gateable devices showed the conventional spin 1/2 Kondo effect. For devices based on cyclo[8]pyrrole, 94 devices were prepared; 13 of these devices proved gateable, and an unconventional Kondo resonance was observed only on one of these latter devices. Using the gateable devices not displaying an unconventional Kondo resonance, we could observe excitation peaks at −14, −7, 7, 14, and 27 mV.

(38) Roch, N.; Florens, S.; Costi, T. A.; Wernsdorfer, W.; Balestro, F. *Phys. Rev. Lett.* **2009**, *103*, 197202.

(39) Anderson, P. W. *Phys. Rev.* **1961**, *124*, 41.

(40) (a) Goldhaber-Gordon, D.; Göres, J.; Kastner, M. A.; Shtrikman, H.; Mahalu, D.; Meirav, U. *Phys. Rev. Lett.* **1998**, *81*, 5225. (b) Parks, J. J.; Champagne, A. R.; Costi, T. A.; Shum, W. W.; Pasupathy, A. N.; Neuscamman, E.; Flores-Torres, S.; Cornaglia, P. S.; Aligia, A. A.; Balseiro, C. A.; Chan, G. K.-L.; Abruña, H. D.; Ralph, D. C. *Science* **2010**, *328*, 1370.

(41) Fitting details: We used the empirical equation of the form $G_K = G_o(1 + (2^{1/\alpha} - 1)(T/T_K)^{\beta})^{-\alpha}$ described by Parks et al.[40b] For the spin 1/2 model, we use the asymptotic values of 0.22 and 2.0 for α and β, respectively. For the spin 1 model, we use 0.75 and 0.5 for α and β, respectively.

(42) Kogan, A.; Granger, G.; Kastner, M. A.; Goldhaber-Gordon, D.; Shtrikman, H. *Phys. Rev. B* **2003**, *67*, 113309.

(43) Kouwenhoven, L. P.; Austing, D. G.; Tarucha, S. *Rep. Prog. Phys.* **2001**, *64*, 701.